

Evaluating the Moisture Susceptibility of Hot-Mix Asphalt with Recycled Crushed Glass

T.B. George

(Council for Scientific and Industrial Research, South Africa)

J.K. Anochie-Boateng

(Council for Scientific and Industrial Research, South Africa)

K.J. Jenkins

(Stellenbosch University, South Africa)

M.F.C. van de Ven

(Technical University of Delft, Netherlands)

Synopsis— The CSIR is currently investigating the suitability of using locally available recycled crushed glass in Hot-Mix Asphalt production. The moisture susceptibility of three dense-graded asphalt mixes incorporating 15% recycled crushed glass (with the first and second mix incorporating hydrated lime and a liquid antistripping additive respectively and the third mix without an antistripping additive) is evaluated in this paper. The tensile strength ratio (TSR), determined from the Modified Lottman test and the stripping inflection point (SIP), determined from the Hamburg wheel tracking test, were the standard parameters used in the moisture susceptibility evaluation. Additionally, a microscopic imaging technique and a new method for SIP determination is proposed in this study to evaluate the stripping potential of the glass-asphalt mixes. The new method for SIP determination appears to be more accurate in evaluating moisture susceptibility than the current standard method and also follows a similar trend to the degree of stripping obtained from the TSR and the microscopic imaging analysis. Preliminary test results show that an antistripping additive is required to meet moisture susceptibility criteria and alleviate stripping in dense-graded glass-asphalt mixes. In particular, moisture susceptibility is improved more using hydrated lime than the liquid antistripping additive.

Keywords— *antistripping additive; glass-asphalt; microscopic imaging; moisture susceptibility; recycled crushed glass; stripping inflection point; tensile strength ratio*

I. INTRODUCTION

Over the past decade, the use of crushed glass in pavement applications has been implemented by various countries in the international community. Such countries include Australia, Canada, Japan, New Zealand, Taiwan, United Kingdom and United States [1-6]. South Africa, however, who on average generates roughly 900 000 tonnes of domestic waste glass each year has made little use of this readily available raw material. National waste information indicates that an estimated 70% of domestic waste glass generated in South Africa was landfilled, while only 30% was recycled [7]. More recently, with national policies mandating the “reuse”, “recycling” and “minimisation” of domestic waste materials, in addition with several economic and environmental benefits [8], it is expected that the use of alternative materials, e.g. recycled waste glass, in road construction will increase.

Crushed waste glass has typically been used as a fine aggregate substitute in Hot-Mix Asphalt (HMA) pavements. Although HMA pavements that have incorporated crushed glass have shown good performance, increased susceptibility to stripping and ravelling have been identified as a primary area of concern [9].

The relatively smooth surface texture of the glass particles may result in insufficient adhesion between the binder and the glass aggregate surface. This can be explained by the ability of the bitumen to wet the glass aggregate. Wetting describes the degree to which a liquid in contact with a solid substrate spreads out, which is quantified by the contact angle that a liquid creates with a solid substrate when both materials come into contact. A contact angle greater than 90° will result in poor wetting while the wetting is better if the contact angle is less than 90° , as shown in Fig. 1. Spreading is said to occur when the contact angle tends to zero. In the case of most siliceous aggregates, which includes crushed glass, which have smooth surface texture, higher contact angles are expected thus reducing wetting of the glass particles, resulting in less adhesion. With fine crushed glass, however, the presence of more fractured faces can improve adhesion purely by increasing the physical area of contact and can additionally prevent an abrupt plane of stress transfer, where the stresses are rather transferred across or into the bitumen, resulting in less stripping than in coarse glass particles [10].

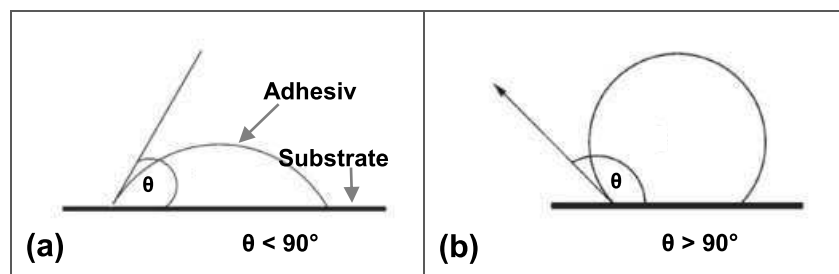


Fig. 1. Schematic representation of adhesive in contact with substrate where a) contact angle less than 90° and b) contact angle greater than 90°

Highly siliceous aggregates are also considered to be poor adherents to the polar groups of bitumen in the presence of water. This is due to the formation of stronger hydrogen bonds between water molecules and silanols (SiOH) than the bond between bitumen polar groups and SiOH groups. The resulting weak binder-aggregate bond can result in stripping.

Although the above physical and chemical behaviour is common with siliceous aggregates, Cheng et al. [11] have demonstrated that irrespective of the strength of the physical or chemical bond between bitumen and aggregate, the bond between water and aggregate is substantially higher. They concluded that the calculated bond strength (ergs/cm²) between water and aggregate (both siliceous and calcareous) is approximately 30% higher than between a variety of bitumen types and the same aggregates. This observation highlights the damaging effects water can have on the adhesive bond (physical or chemical) between aggregate (siliceous or calcareous) and bitumen.

The use of antistripping additives is said to modify the physical and chemical properties of the aggregate and bitumen, thereby improving the durability and strength of the interfacial bond between the two surfaces. Through the addition of hydrated lime (Ca(OH)₂), insoluble calcium organic salts are formed when the Ca²⁺ ions from the lime react with the carboxylic acids and 2-quinolones from the bitumen. The formation of these strong bonds contribute to improved adhesion [12]. Schmidt and Graf [13] have indicated that improved adhesion can also be achieved with hydrated lime due to the migration of Ca²⁺ ions to the surface of the aggregate, where hydrogen, sodium, potassium, or other cations are replaced. This results in calcium rich bonding sites for bitumen acidic groups. Additionally, studies conducted by Robert et al. [14] have revealed that hydrated lime forms strong bonds with most siliceous aggregates through the formation of a calcium silicate crust on the surface of the aggregate which has adequate porosity for binder penetration. Amine based liquid anti-stripping additives are also known to improve the adhesion of bitumen with siliceous aggregates. The long hydrocarbon chain of the amine acts as a bridge between the siliceous aggregate and the bitumen surface, encouraging a strong bond between the two surfaces [15].

The objective of this paper is to determine the influence of 15% recycled crushed glass on the moisture susceptibility of a conventional South African HMA mix (i.e. 10 mm nominal maximum particle size (NMPS) medium dense-graded asphalt wearing course mix). The effect of selected antistripping additives on the moisture susceptibility of three such glass-asphalt mixes (referred to as GA Mix 1, GA Mix 2 and GA Mix 3) is assessed using the standard tensile strength ratio and the stripping inflection point parameters. Additionally, a microscopic imaging technique which quantifies the area of stripping, as well as a new method to determine the stripping inflection point from the Hamburg wheel tracking test is used to assess the moisture susceptibility of the glass-asphalt mixes.

II. MATERIALS AND PROPERTIES

A. Aggregate and Design Aggregate Grading

The same aggregates (andesite 9.5 mm, andesite 6.7 mm, andesite crusher dust, granite crusher sand and mine sand) that were used in the conventional South African HMA mix (control mix) were used to manufacture the glass-asphalt mixes. The granite crusher sand was partially substituted with 15% of recycled crushed glass due to the similar particle size distribution of both materials. The

combined grading of the individual aggregates, crushed glass material and mineral filler was optimized to represent a similar design aggregate grading to the control mix. The design aggregate grading of the glass-asphalt mix is plotted on a 0.45 power chart, presented in Fig. 2. It can be observed that the design grading falls within the grading control points specified in the South African mix design guideline for a 10 mm NMPS dense-graded asphalt mix [16].

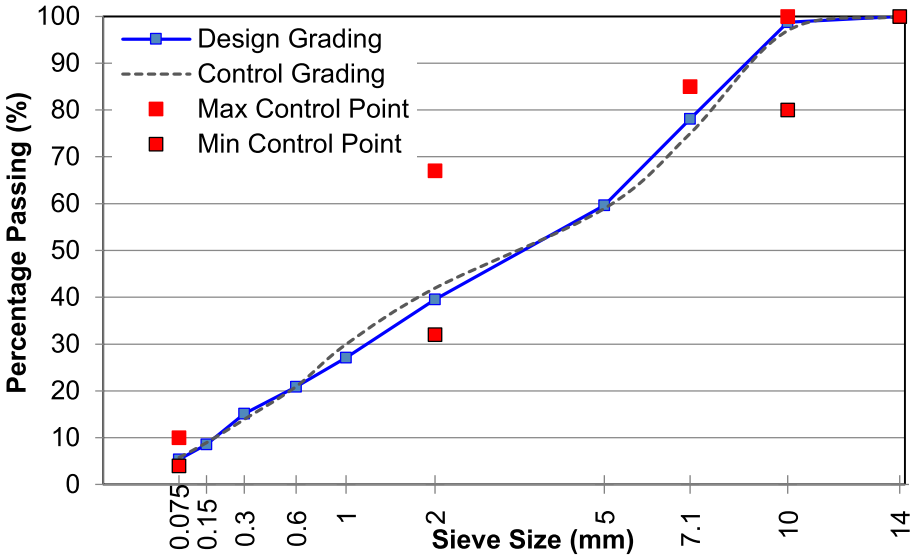


Fig. 89. Design aggregate grading of glass-asphalt mix on 0.45 power chart

B. Recycled Crushed Glass

The recycled crushed glass was procured from a glass manufacturing plant located in the Gauteng province. The morphology of the crushed glass material was examined by Scanning Electron Microscopy (SEM), as shown in Fig. 3. It can be observed that the crushed glass material consists of mostly fine angular particles with fine to coarse textured features present on the surfaces of the glass particles. Furthermore, due to the fine particle size distribution of the crushed glass material, reduced quantities of particles with sharp edges as well as reduced quantities of elongated particles can be observed.

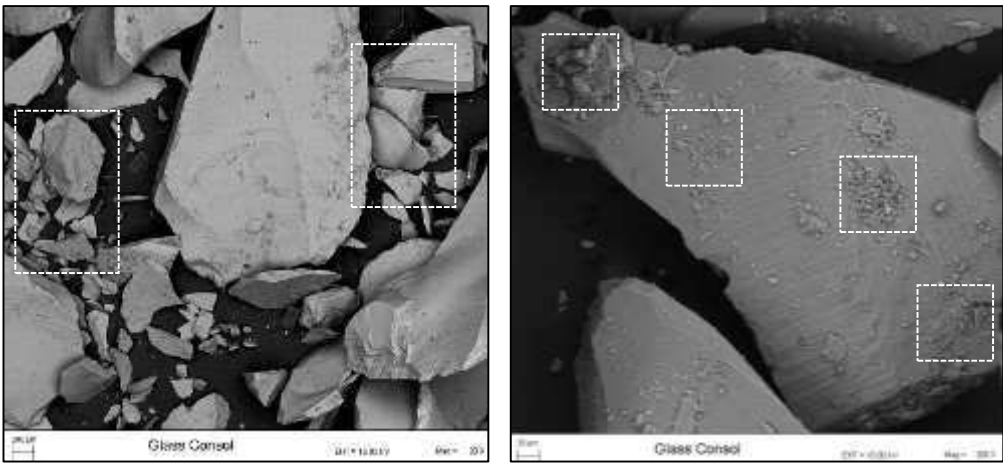


Fig. 90. *Fine angular recycled crushed glass particles with textured surface features*

The particle size distribution of the crushed glass is reported in Table 1 and represents a fine continuous grading with a maximum particle size (MPS) of 5mm.

TABLE I. PARTICLE SIZE DISTRIBUTION OF RECYCLED CRUSHED GLASS

| Sieve Size (mm) | 5 | 2 | 1 | 0.6 | 0.3 | 0.15 | 0.075 |
|----------------------------|-----|----|----|-----|-----|------|-------|
| Recycled Crushed Glass (%) | 100 | 82 | 46 | 27 | 15 | 8 | 4.3 |

Additional physical properties of the recycled crushed glass are reported in Table 2. It should be mentioned that the angularity of the crushed glass (51%) was higher than the fine andesite (44.6%) and fine granite (45.0%) aggregates in the FAA test. An X-Ray Diffraction (XRD) analysis conducted on the crushed glass indicated that on average more than 90% of the recycled crushed glass sample consisted of amorphous silica while less than 10% consisted of crystalline silica. The source of recycled crushed glass, therefore, demonstrates a high degree of purity, which is also apparent from the sand equivalency test results reported in Table 2. Additionally, the chemical composition of the crushed glass was characterised by an X-ray fluorescence (XRF) analysis which indicated that 71.7% of the crushed glass material consists of SiO₂.

PHYSICAL PROPERTIES OF RECYCLED CRUSHED GLASS

| Physical Property | Test Method | Result | Criteria |
|---------------------------------|-----------------------|--------|-----------------------|
| Bulk Relative Density | SANS 3001-AG21 (2014) | 2.451 | - |
| Apparent Relative Density | | 2.518 | - |
| Water Absorption | | 0.5 % | Max. 1.5% |
| Fine Aggregate Angularity (FAA) | ASTM C1252 (2003) | 51 % | Min. 45% ¹ |
| Sand Equivalency | SANS 3001-AG5 (2014) | 89 % | Min. 50% |

¹AASHTO M323 (2013) Superpave mix design specification

C. Antistripping Additives

Hydrated lime (1% by mass of dry aggregate) and an amine-based liquid additive (0.5% by volume of binder) was applied to GA Mix 1 and GA Mix 2 respectively. The incorporation of 1% hydrated lime was based on the maximum specified amount allowed for inclusion in dense-graded asphalt mixes in South Africa [16]. The liquid additive selected for this study is often used as an adhesion promoter in hot-mix asphalt production in South Africa.

D. Mineral Filler

The hydrated lime also constituted the filler component in GA Mix 1. To investigate the effect of the liquid antistripping additive on the moisture susceptibility of GA Mix 2 as well as similar effects on the moisture susceptibility of GA Mix 3 without an antistripping additive, the mineral filler in GA

Mix 2 and 3 consisted of 1% (by mass of dry aggregate) of baghouse fines instead of hydrated lime. Although the type of mineral filler varied, the design grading of all three mixes was not affected due to similar particle size distribution of both filler components.

E. Bitumen

The same binder, i.e. 50-70 penetration grade binder with penetration (25°C, 100 g, 0.1 mm) of 65 and softening point after Rolling Thin Film oven (RTFO) aging at 47°C, that was utilised in the control mix was used to prepare the glass-asphalt mixes. The properties of the binder conform to the South African National Standard 4001-BT1 requirements [17].

III. LABORATORY TESTING PROGRAM

A. Mix Design and Optimum Binder Content

The glass-asphalt mix design was conducted in accordance with the South African mix design guideline for dense-graded asphalt mixes [16]. The mix design method specifies the optimum binder content to be established at 4% air voids in the mix. As per this criterion, an optimum binder content of 5.4% for all three glass-asphalt mixes was determined. The volumetric properties obtained at the optimum binder content for the glass-asphalt mixes are summarised in Table 3.

VOLUMETRIC PROPERTIES OF GLASS-ASPHALT MIXES AT OPTIMUM BINDER CONTENT

| Glass-Asphalt Mix | Voids In Mix (%) | Voids in Mineral Aggregate (%) | Voids Filled with Binder (%) |
|--------------------------|-------------------------|---------------------------------------|-------------------------------------|
| GA Mix 1 | 4 | 15.6 | 73.5 |
| GA Mix 2 | 4 | 15.6 | 74.0 |
| GA Mix 3 | 4 | 15.7 | 73.8 |
| Criteria | 4 | Min. 15 | 65-75 |
| Pass/Fail | Pass | Pass | Pass |

B. Mix Sample Preparation

The glass-asphalt samples were manufactured at a mixing temperature of 150°C and a compaction temperature of 135 °C. Prior to compaction, the asphalt mixtures were shot-term aged for 4 hours at 135 °C, to simulate the aging that takes place during the production process in an asphalt plant and transport to site. The Modified Lottman and Hamburg wheel tracking test (HWTT) test samples were compacted to dimensions of 100 mm diameter by 60 mm height and 150 mm diameter by 60 mm height respectively. The samples were compacted at the determined optimum binder content to the target field air voids content of approximately 7%. Compaction of the samples to the target height and air voids were typically achieved after 90 to 120 gyrations using a Superpave Servopac gyratory compactor in accordance with AASHTO T312-15 [18].

C. Modified Lottman Test

The Modified Lottman test is the standard laboratory test adopted in South Africa to evaluate the durability of dense-graded asphalt mixes [16] and is conducted in accordance with ASTM D4867M-09 [19].

Six gyratory compacted samples, for each mix, were divided into two subsets, where one subset was kept dry while the other underwent a partial saturation and freeze-thaw conditioning process. The conditioned (wet) and unconditioned (dry) subsets were then brought to a constant temperature (25°C) prior to indirect tensile strength (ITS) testing. The test specimens were placed in the loading apparatus and the loading strips were then centrally positioned on the vertical diametrical plane. A displacement rate of 50 mm/min was applied. From the load-displacement curve, the maximum load required to fracture the specimens was determined. This maximum load was used to calculate the ITS for each subset. In the results the mean value of three samples is given.

D. Hamburg Wheel Tracking Test

The Hamburg Wheel Tracking Test (HWTT) is currently used in South Africa as the standard laboratory test to evaluate the “combined effects of moisture damage and rutting potential” of asphalt mixes [16] and is conducted according to AASHTO T 324-14 [20].

The specimen setup as described in the specification allows for testing to be conducted on either a slab specimen or a pair of cylindrical specimens. For this study, a pair of cylindrical compacted specimens for each mix were mounted together and then submerged in the water bath of the Hamburg wheel tracking device at 50°C for 30 minutes prior to testing. The adjoined specimens were thereafter subjected to a moving wheel load of 703 N which covers a distance of 230 mm in one direction along the surface of the cylindrical specimens. During testing, the rut depth was measured along the surface of the adjoined cylindrical specimens using a profilometer and the maximum rut depth obtained at the recorded number of wheel passes was used as the output data for analysis and reporting of the HWTT results.

IV. MOISTURE SUSCEPTIBILITY EVALUATION

A. Moisture Susceptibility Evaluation Using Modified Lottman Test

The Modified Lottman test was used in this study to assess the moisture susceptibility of GA Mix 1, 2 and 3. The test uses an indirect tensile strength (ITS) ratio to rank mix sensitivity to moisture damage, as described next.

INDIRECT TENSILE STRENGTH

The average ITS results of the wet and dry subsets are reported in Table 4. In South Africa, the minimum ITS criteria is 800 kPa at 25°C. However, a recent study has shown that ITS values lower than 1000 kPa may have a tendency to demonstrate reduced rutting resistance in the field while ITS values higher than 1700 kPa may demonstrate brittleness and low flexibility [21]. It can be observed that the dry ITS results for all three glass-asphalt mixes meet the minimum criteria (i.e. 800 kPa) while only GA Mix 1 exceeds 1 000 kPa.

It was also interesting to note that GA Mix 2, which contains a liquid antistripping additive, indicated the lowest dry strength in comparison with GA Mix 1 and 3. Although a larger reduction in dry strength was noted, the percentage reduction in strength of the conditioned subset of GA Mix 2 (20%) was not as pronounced as in the case of GA Mix 3 (24%); which was expected due to the absence of an antistripping additive in GA Mix 3. The liquid additive may have an influence on the bitumen stiffness

in the asphalt mixes resulting in a lower strength at this temperature and displacement rate, but the moisture susceptibility may improve.

TENSILE STRENGTH RATIO

The stripping potential of the glass-asphalt mixes was evaluated by the tensile strength ratio (TSR). The TSR is determined from the ratio of the average ITS of the wet subset to the average ITS of the dry subset [19].

In South Africa a minimum TSR of 0.8 for asphalt wearing courses is specified [16]. The results in Table 4 show that GA Mix 1 and 2 meet the minimum TSR criteria, whereas GA Mix 3 fails to comply with the specified requirement. Based on the TSR as an indicator of moisture susceptibility; it is anticipated that GA Mix 1 will be less susceptible to moisture damage than GA Mix 2, while GA Mix 3 is expected to demonstrate the least resistance to moisture damage.

TENSILE STRENGTH RATIO OF GLASS-ASPHALT MIXES

| Parameter | GA Mix 1 | | GA Mix 2 | | GA Mix 3 | |
|-------------------|------------|------------|------------|------------|------------|------------|
| | Dry Subset | Wet Subset | Dry Subset | Wet Subset | Dry Subset | Wet Subset |
| Average ITS (kPa) | 1106 | 982 | 867 | 692 | 950 | 772 |
| TSR | 0.89 | | 0.80 | | 0.76 | |

B. Moisture Susceptibility Evaluation Using Microscopic Imaging

A microscopic imaging analysis was implemented in this study to assess the degree of stripping that had occurred in each of the three glass-asphalt mixes. This analysis was used to eliminate visual judgment and biased interpretation associated with the ASTM D4867M requirement of visual inspection and reporting. Additionally, this method can be used to verify the determined TSR results, considering that the prediction of moisture susceptibility from the Modified Lottman test remains empirical.




The analysis was conducted on the Modified Lottman test samples. One fractured sample from the wet subset of each mix was examined under a stereo microscope at a 6x zoom magnification. In order to obtain a representative area, six sections of dimension 22.05 mm (width) by 14.68 mm (height) each spanning over the cross-sectional area of the fractured sample were examined under the microscope.

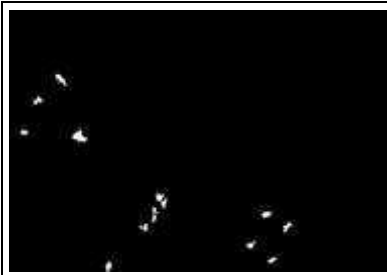
The microscopic sections were captured by an integrated digital camera and the resulting images were imported into ImageJ, the public domain Java Image processing program, inspired by National Institute of Health (NIH). In ImageJ, the captured images were converted to 8-bit grayscale images

which consist of 256 levels of grey intensity per pixel that range from 0 (black) to 255 (white). The variation in grey intensity levels is dependent on the density of each component material in the mix. Dense materials are represented by the brighter regions while low density materials are represented by the darker regions. As such, in this analysis the exposed aggregates correspond to the brighter regions and the bituminous coated aggregates, mastic and voids correspond to the darker regions. Since the pixel grey values of the exposed aggregates and the remaining material phases (i.e. bituminous coated aggregates, mastic and voids) were distinctly different from each other, a threshold value of 65 was easily selected to distinguish between the two regions. This threshold value was considered to be most accurate in identifying the areas of stripping and was consistently applied for all the three mixes for realistic comparison.

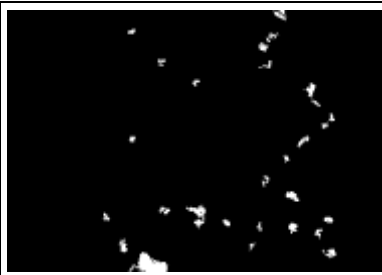
The applied threshold level converts the image to a binary image, where all pixels in the greyscale image greater than the threshold value are replaced with the value 255 (white) and the remaining pixels with the value 0 (black). The binary images were used to quantify the degree of stripping by measuring the area of white pixels (area of exposed aggregates) as a ratio to the area of sum of white and black pixels² (total sample surface area) for each mix. The area measurement of white and black pixels was automatically computed in the software. The results of this analysis are provided in Fig. 4.

The results show a clear variation in the degree of stripping with the addition of both antistripping additives. A significant reduction in the area of white pixels (stripped areas) can be observed for GA Mix 1 and 2 in comparison with GA Mix 3. The total area of white pixels reduces from approximately 47% (GA Mix 3) to less than 10% (GA Mix 1 and 2). These results confirm the effectiveness of antistripping additives in significantly improving the moisture susceptibility of glass-asphalt mixes. Moreover, the addition of hydrated lime appears to reduce the stripped areas more than the liquid antistripping additive; although a major distinction was not apparent from the microscopic images.

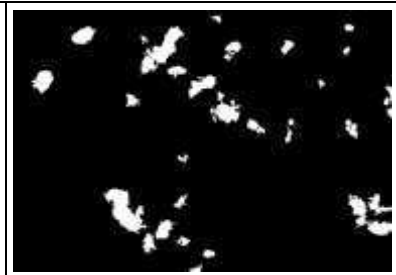
| GA Mix 1 | GA Mix 2 | GA Mix 3 |
|--|--|---|
|  <p data-bbox="103 1552 488 1664"> Area of white pixels = 3.6 mm² Area of stripping = 1.1% </p> |  <p data-bbox="558 1552 943 1664"> Area of white pixels = 2.1 mm² Area of stripping = 0.6% </p> |  <p data-bbox="1029 1552 1414 1664"> Area of white pixels = 10.4 mm² Area of stripping = 3.2% </p> |



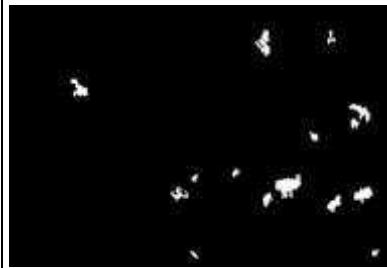
Area of white pixels = 1.9 mm²
Area of stripping = 0.6%



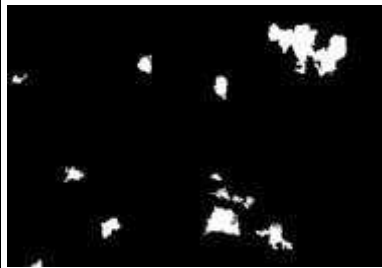
Area of white pixels = 5.2 mm²
Area of stripping = 1.6%



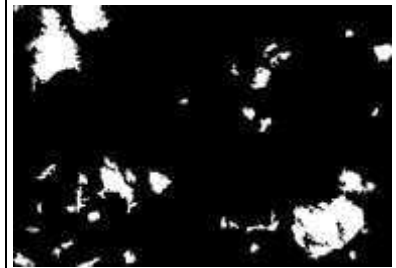
Area of white pixels = 18.3 mm²
Area of stripping = 5.7%



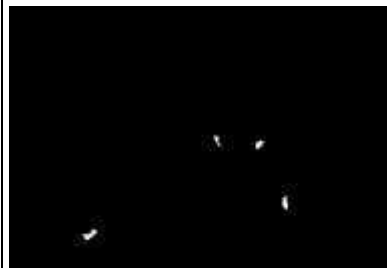
Area of white pixels = 5.1 mm²
Area of stripping = 1.6%



Area of white pixels = 13.3 mm²
Area of stripping = 4.1%



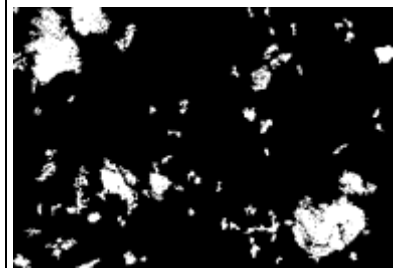
Area of white pixels = 30.9 mm²
Area of stripping = 9.6%



Area of white pixels = 0.6 mm²
Area of stripping = 0.2%



Area of white pixels = 1.4 mm²
Area of stripping = 0.4%



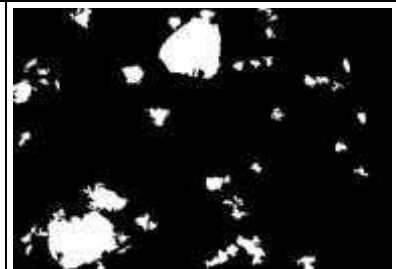
Area of white pixels = 37.2 mm²
Area of stripping = 11.5%



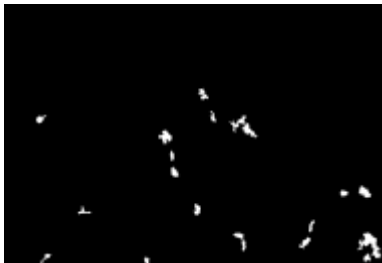

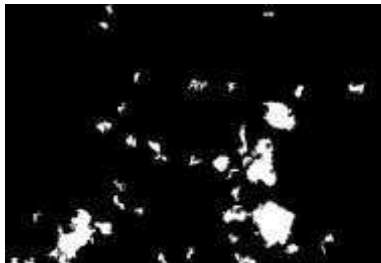
Area of white pixels = 4.9 mm²
Area of stripping = 1.5%



Area of white pixels = 4.9 mm²
Area of stripping = 1.5%



Area of white pixels = 33.2 mm²
Area of stripping = 10.3%

| | | |
|---|---|---|
|  |  |  |
| Area of white pixels = 3.9 mm ² Area of stripping = 1.2% | Area of white pixels = 5.4 mm ² Area of stripping = 1.7% | Area of white pixels = 19.6 mm ² Area of stripping = 6.1% |
| Total Area of Stripping | | |
| 6.2% | 9.9% | 46.4% |

²Total area of black and white pixels = 323.34 mm²

Fig. 91. Microscopic imaging analysis of glass-asphalt mixes

c. Moisture Susceptibility Evaluation Using Hamburg Wheel Tracking Test

In the HWTT, the maximum rut depth obtained at the recorded number of wheel passes is used as the output data for analysis. As illustrated in Fig. 5. A typical HWTT output curve can be divided into three main phases [22], as described below:

- Post compaction phase: the specimen is consolidated within the post compaction phase which takes place when the mix is densified by the wheel load and a significant decrease in the air voids occurs. This phase is assumed to take place during the first 1000 wheel passes [22].
- Creep phase: the creep phase occurs primarily as a result of the permanent deformation of the asphalt mix under loading and is represented by an approximately constant rate of increase in rut depth with wheel pass.
- Stripping phase: the stripping phase starts after water penetrates through the binder-aggregate interface and the bond between the two components start to degrade resulting in an accelerated increase in rut depth with wheel pass. The rut depth accumulated in this phase is a contribution mainly from moisture damage (stripping) as well as from further permanent deformation under loading.

AASHTO T324 requires the following test parameters to be determined from the aforementioned phases in order to quantify the resistance of a mix to moisture damage (stripping) [20]. The test parameters are graphically illustrated in Fig. 5

- Creep slope (“first portion” in (1))
- Stripping slope (“second portion” in (1))
- Stripping Inflection Point (SIP): The SIP is the graphical point on the HWTT curve at which the creep slope intersects the stripping slope. This point on the curve is representative of the number of wheel passes where the rut depth suddenly increases, primarily due to the stripping of the binder

from the aggregate [22]. The SIP is therefore hypothesised to represent the onset of stripping and is indicative of the resistance of an asphalt mix to moisture damage. The SIP, with respect to the number of wheel passes, is defined in AASHTO T 324 as shown in (1) [20].

$$SIP = \frac{\text{Intercept (second portion)} - \text{Intercept (first portion)}}{\text{Slope (first portion)} - \text{Slope (second portion)}} \quad (1)$$

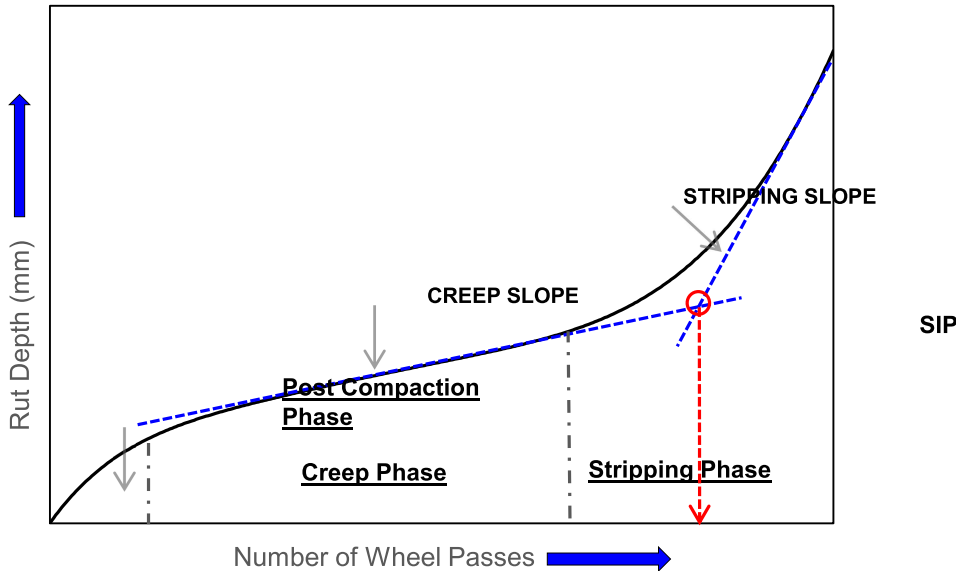


Fig. 92. Typical HWTT output curve with test parameters

Currently, the SIP at a certain number of wheel passes is widely used as the main HWTT parameter to evaluate the moisture susceptibility of asphalt mixes. Extensive research conducted by the Colorado Department of Transportation (CDOT) has indicated that asphalt mixes with SIP values greater than 10 000 passes demonstrated good pavement performance while for pavements that lasted 1 year, the SIP values were less than 3 000 passes [23]. It should be noted that the compliance criteria for stripping in South Africa allows for a minimum of 10 000 passes to the SIP [16].

Although the SIP has been increasingly used to evaluate moisture susceptibility, it has been noted that analysis and reporting of the SIP and the aforementioned test parameters (i.e. creep slope and stripping slope) are not clearly and consistently defined as well as not standardised in AASHTO T 324. Visually selecting the “first portion” and “second portion” and manually plotting straight lines from the creep phase and stripping phase for the determination of the resultant slopes and intercepts is vague and may thus introduce variation during SIP calculations. Moreover, the post compaction phase is assumed to occur within the first 1000 cycles which is mostly used as the starting point to plot the creep slope for determination of the SIP.

PROPOSED NEW METHOD FOR MOISTURE SUSCEPTIBILITY EVALUATION

To improve the evaluation of mix moisture susceptibility, a new analysis approach is proposed in this study by curve fitting the HWTT results for the complete output of rut depth against number of

wheel passes. This approach introduces a new SIP parameter to evaluate the resistance of the glass-asphalt mixes to moisture damage. In addition, the new approach is compared with the current analysis procedure in AASHTO T 324 in order to assess its ability to effectively evaluate the moisture susceptibility performance of the glass-asphalt mixes in the HWTT.

For this analysis, a 6-degree polynomial function is used to fit the HWTT output data for rut depth versus number of wheel passes, as described in (2).

$$RD_N = aN^6 + bN^5 + cN^4 + dN^3 + eN^2 + fN + C \quad (2)$$

Where:

RD_N = Rut depth after N wheel passes (mm)

N = Number of wheel passes

a, b, c, d, e, f and C = 6-degree polynomial coefficients

The polynomial functions used to fit the HWTT output data for GA Mix 1, 2 and 3 are provided in Table 5 and illustrated in Fig. 5. Accurate prediction of the measured rut depth can be observed, with a coefficient of determination (R^2) value of 0.99 for all three mixes.

FITTED HWTT DATA FOR GLASS-ASPHALT MIXES

| Mix | Fitted HWTT Curve Equation | R^2 |
|------|---|-------|
| GA 1 | $RD = 3.9E-25N^6 + 8.3E-20N^5 - 3.2E-15N^4 + 5.3E-11N^3 - 4.7E-07N^2 + 2.6E-03N + 0.4$ | 0.999 |
| GA 2 | $RD = -1.2E-22N^6 + 5.7E-18N^5 - 1.0E-13N^4 + 8.5E-10N^3 - 3.6E-06N^2 + 7.8E-03N + 2.5$ | 0.993 |
| GA 3 | $RD = -4.7E-23N^6 + 2.4E-18N^5 - 4.6E-14N^4 + 4.3E-10N^3 - 2.0E-06N^2 + 5.2E-03N + 0.8$ | 0.999 |

It can be observed from the fitted curves that GA Mix 1, 2 and 3 experienced the post-compaction phase (Phase 1), creep phase (Phase 2) and stripping phase (Phase 3) during the test. The rut depth in the post compaction phase increases rapidly within the first 2 000 cycles and thereafter reaches an approximately constant rate of increase in rut depth, represented by the creep phase. It may therefore not be reasonable to assume that Phase 1 occurs within 1000 cycles as the number of cycles accumulated in this phase varies depending on when the rate of deformation stabilises. This variance may be attributed to differences in air void content, method of compaction, workability of the mix, mix type, performance grade of the binder etc. for a particular mix.

Following the creep phase, it can be observed that there is a rapid increase in the rut depth. It is apparent that this accelerated increase in rut depth occurs where the mix transitions from the creep phase to the stripping phase. Graphically, this transition is represented at the point where the curvature of the fitted HWTT curve changes from negative to positive. To determine the point at which the curvature changes from negative to positive, the second derivative of (2) is determined, as described in (3).

$$\frac{d^2RD}{dN^2} = 30aN^4 + 20bN^3 + 12cN^2 + 6dN + 2e \quad (3)$$

The new SIP parameter (SIP_{New}) is determined by setting (3) to zero and solving for the number of wheel passes (N). The corresponding number of wheel passes at this inflection point signifies the maximum number of wheel passes that can be resisted by the asphalt mix in the HWTT before adhesive failure at the binder-aggregate interface occurs. As such, mixes with higher SIP_{New} values is expected to be less moisture susceptible as opposed to those with lower SIP_{New} values.

The HWTT results for all three glass-asphalt mixes were evaluated using the SIP_{New} parameter as a moisture susceptibility indicator. A SIP_{New} of 10 636, 10 101 and 9 731 wheel passes were obtained for GA Mix 1, 2 and 3 respectively. The results are presented graphically in Fig. 6.

STANDARD METHOD FOR MOISTURE SUSCEPTIBILITY EVALUATION

According to AASTO T324, quantification of the SIP is defined in (1). As previously mentioned, AASHTO T324 does not define how to identify the “first portion” (creep phase) and the “second portion” (stripping phase) in order to plot the respective slopes.

In this study, the “first portion” was identified after the post compaction phase, where deformation rate was approximately constant. The number of cycles and rut depth in this portion of the fitted curve was used to calculate the slope and intercept of the straight line plotted through the creep phase. The start of the “second portion” was identified where the curvature of the fitted curve changed from negative to positive. The stripping slope was obtained by drawing a tangential line at the location of the maximum rut depth in this portion of the fitted curve. The intersection of the two straight lines was then used to calculate the stripping inflection point ($SIP_{Standard}$) for GA Mix 1, 2 and 3 based on (1). The results are summarised in Table 6 and graphically presented in Fig. 6.

DETERMINATION OF SIP ACCORDING TO AASHTO T324

| GA Mix 1 | GA Mix 2 | GA Mix 3 |
|--|---|---|
| $SIP = \frac{Intercept (second\ portion) - Intercept (first\ portion)}{Slope (first\ portion) - Slope(second\ portion)}, [20]$ | | |
| $SIP = \frac{(-69.86 - 3.76)}{(0.00054 - 0.00585)} = 13\ 864$ | $SIP = \frac{(-41.35 - 6.87)}{(0.00102 - 0.00518)} = 11\ 582$ | $SIP = \frac{(-35.69 - 3.27)}{(0.00110 - 0.00435)} = 11\ 976$ |

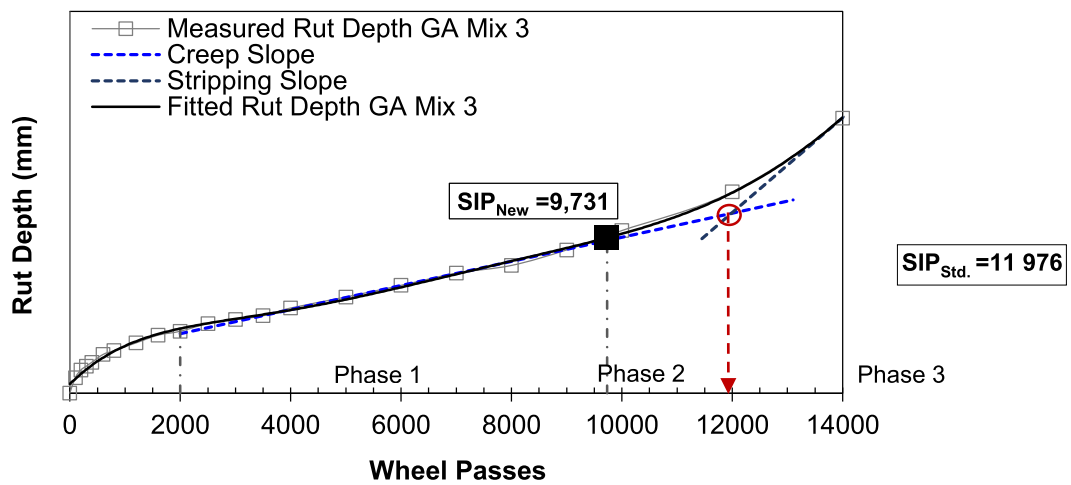
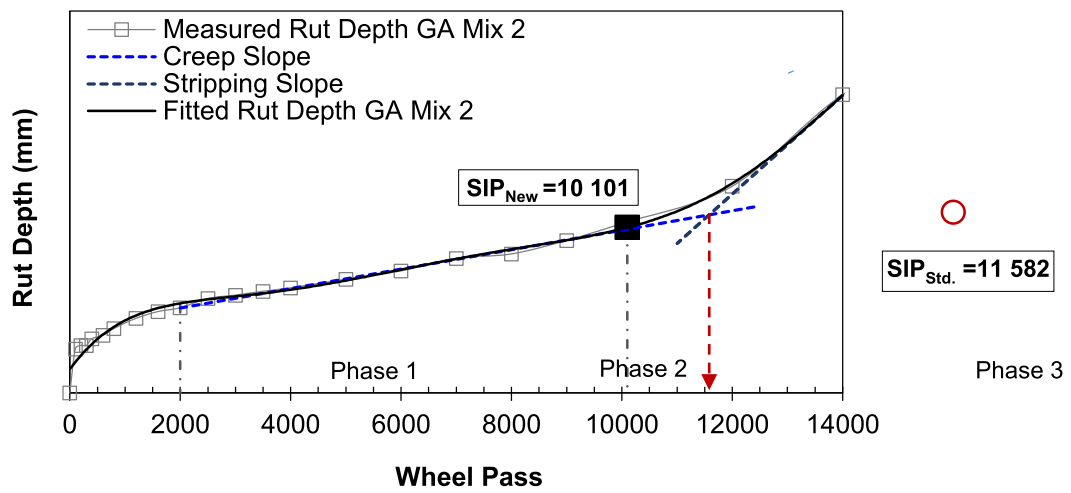
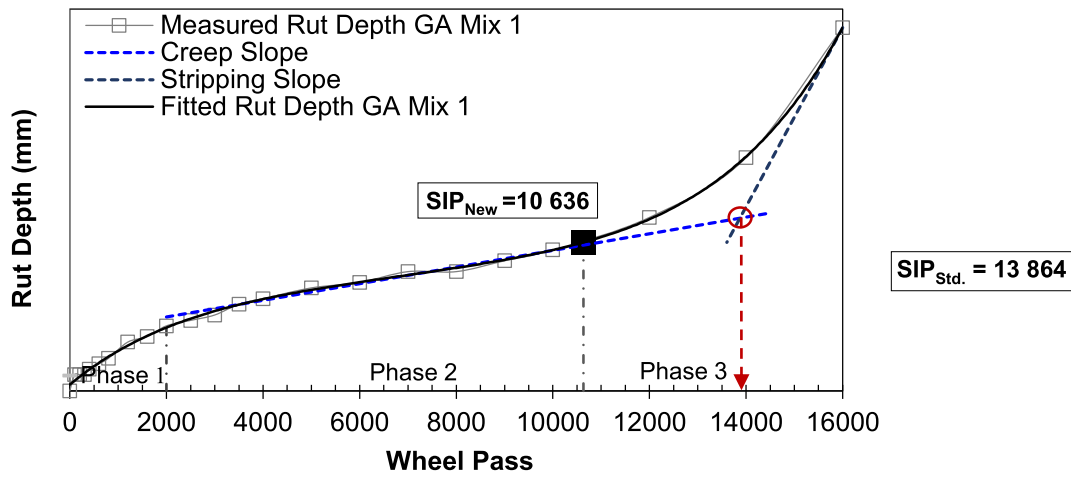


Fig. 93. *Moisture susceptibility evaluation of glass-asphalt mixes using stripping inflection point*

RESULTS AND DISCUSSIONS

From the results, it can be observed that the $SIP_{Standard}$ value for GA Mix 3 (11 976 wheel passes) is higher than the $SIP_{Standard}$ value for GA Mix 2 (11 582 wheel passes). This is quite surprising as GA Mix 3 does not incorporate an antistripping agent but appears to have a greater resistance to moisture damage than GA Mix 2, as indicated by a higher $SIP_{Standard}$ value. Since it is expected that the absence of an antistripping additive, particularly in glass-asphalt mixes, will cause early adhesive failure and stripping in the mix, it is unlikely that GA Mix 3 will demonstrate better resistance to moisture damage. The $SIP_{Standard}$ results are also contrary to the microscopic images, which revealed much more uncovered surface areas of both aggregates and glass particles in GA Mix 3, while signs of minor stripping were only visible on the tested samples of GA Mix 2. Moreover, the calculated $SIP_{Standard}$ value of GA Mix 3 (i.e. 11 976 wheel passes) relative to the minimum SIP criterion for good moisture susceptibility performance (i.e. >10 000 wheel passes) further validates inconsistency of the standard SIP parameter in effectively evaluating mix moisture susceptibility. In this regard, it is evident that the proposed new SIP parameter is more effective in evaluating mix moisture susceptibility than the standard method of evaluation, with GA Mix 1 and 2 resulting in SIP_{New} values greater than 10 000 passes while GA mix 3 failing to meet the minimum SIP criterion.

The SIP_{New} results are also consistent with the degree of moisture damage obtained from the TSR parameter and the microscopic imaging analysis, as indicated in Table 7. A summary of the moisture susceptibility ranking of GA Mix 1, 2 and 3, using the TSR, microscopic imaging, standard SIP and new SIP as ranking parameters, is presented. A ranking of 1 to 3 indicates least (1) to most (3) moisture susceptible.

MOISTURE SUSCEPTIBILITY RANKING OF GLASS-ASPHALT MIXES

| Glass-Asphalt Mix | Performance Ranking | TSR ³ | Microscopic Image Analysis | $SIP_{Standard}^4$ | SIP_{New}^4 |
|-------------------|---------------------|------------------|----------------------------|--------------------|---------------|
| GA Mix 1 | 1 | 0.89 (1) | 6.2% (1) | 13 864 (1) | 10 636 (1) |
| GA Mix 2 | 2 | 0.80 (2) | 9.9% (2) | 10 893 (3) | 10 101 (2) |
| GA Mix 3 | 3 | 0.76 (3) | 46.4% (3) | 11 976 (2) | 9 731 (3) |

³ Min. TSR criteria (South Africa) = 0.8

⁴ Min. SIP criteria (South Africa) = 10 000 passes

It is evident from the summary that all parameters appear to effectively rank GA Mix 1 as least susceptible to moisture damage. Although GA Mix 2 meets the minimum TSR and SIP criteria for moisture susceptibility, it is evident that the hydrated lime in GA Mix 1 is more effective than the liquid antistripping additive in GA Mix 2 in resisting moisture damage. Furthermore, it can be observed that

GA Mix 3, which does not contain an antistripping additive, is ranked (by all parameters except SIP_{Standard}) as most susceptible to moisture damage and additionally does not meet the moisture susceptibility criteria.

V. CONCLUSIONS AND RECOMMENDATIONS

It can be concluded from this study that an antistripping additive is required to meet moisture susceptibility criteria and alleviate stripping in medium dense-graded asphalt mixes consisting of 15% recycled crushed glass. Additionally, it can be concluded that hydrated lime is more effective than the liquid antistripping additive in alleviating stripping. In this regard, the liquid antistripping additive, which is known to be commonly used in HMA production in South Africa, may not be as effective in such non-traditional asphalt mixes, while also reducing the strength of the mix.

Furthermore, the proposed new method to determine the SIP parameter is more effective in evaluating mix moisture susceptibility than the standard method of evaluation which demonstrates inconsistency in the calculated SIP value. This is based on vague and biased interpretation associated with manually plotting straight lines from the creep and stripping phase during SIP calculations in the current standard method as opposed to the proposed new method which models the HWTT output data to determine the SIP. Unlike the standard SIP parameter, the new SIP parameter shows consistency with the degree of moisture damage obtained from the TSR parameter and the microscopic imaging analysis, determined from the Modified Lottman test.

It is, however, recommended that future research into the correlation between the proposed new method for SIP determination and the SIP compliance criterion with glass-asphalt pavements of known stripping performance be conducted. In addition, the microscopic imaging techniques conducted to evaluate mix moisture susceptibility is capable of providing an accurate representation of the degree of stripping and furthermore eliminates visual judgment and biased interpretation associated with the current standard of visual inspection and reporting. This method is also recommended to validate the Modified Lottman test results.

ACKNOWLEDGEMENT

The authors wish to acknowledge the Council for Scientific and Industrial Research (CSIR) through its R&D office for funding this research through Parliamentary Grant (PG) Funding.

REFERENCES

- [1] Yamanaka, M., Gotoh, K., Saruwatari, M. & Mochishita, T., 2001. *Thermal and mechanical Properties of Glass Cullet Mixed with Asphalt as Low-Exothermic Pavement Material*. Japan: Nagasaki University.
- [2] Su, N. & Chen, J.S., 2002. Engineering properties of asphalt concrete made with recycled glass. *Resources, Conservation and Recycling*, 35, pp.259-74.

- [3] Dane County Department of Public Works, 2003. *Resuse/Recycling of Glass Cullet for Non-Container Uses*. Wisconsin, USA.
- [4] Arnold, G., Werkemeister, S. & Alabaster, D., 2008. *The effect of adding recycled glass on the performance of basecourse aggregate*. Research Report 351.40 pp. NZ Transport Agency.
- [5] Australian Government: Department of Sustainability, Environment, Water, Population and Communities, 2011. *National Waste Policy Case Study*. Commonwealth of Australia.
- [6] Andela, C. & Sorge, E.V., n.d. *Handbook of Alternative Uses for Recycled Glass*.
- [7] Department of Environmental Affairs, 2012. *National Waste Information Baseline Report*.
- [8] George, T.B. and Anochie-Boateng, J.K., 2016. Assessment on the sustainable use of alternative construction materials as a substitute to natural aggregates. *4th International Conference on Sustainable Construction Materials and Technologies*. Las Vegas, USA.
- [9] Federal Highway Administration, 1998. *User Guidelines for Waste and By-product Materials in Pavement Construction*. FHWA-RD-97-148, Report No. 480017, Guideline Manual.
- [10] Pocius A. V., 1997. *Adhesion and Adhesives Technology*. Hanser Publications, Ohio, USA.
- [11] Cheng, D., Little, D.N., Lytton, R.L. & Holste, J.C., 2002. Surface Energy Measurements of Asphalt and Its Application to Predicting Fatigue and Healing in Asphalt Mixtures. *Transportation Research Record: Journal of the Transportation Research Board*, 1810, pp.44-53.
- [12] European Lime Association, 2010. *Hydrated lime: A proven additive for durable asphalt pavements*. Brussels, Belgium.
- [13] Schmidt, R. J., & P. E. Graf., 1972. The Effect of Water on the Resilient Modulus of Asphalt Treated Mixes. *Association of Asphalt Paving Technologists*, 41, pp.118–162.
- [14] Roberts, F.L. et al., 1996. *Hot Mix Asphalt Materials, Mixture Design and Construction*. 2nd ed. Lanham, Maryland: National Asphalt Pavement Association Research and Education Foundation.
- [15] Tarrer, A.R. & Wagh, V., 1991. *The Effect of the Physical and Chemical Characteristics of the Aggregate on Bonding*. SHRP Report A/UIR-91-507. Washington, D.C.: Strategic Highway Research Program.
- [16] Sabita, 2016. Sabita Manual 35/TRH8: *Design and Use of Asphalt in Road Pavements*. South Africa.
- [17] South African Bureau of Standards (SABS), 2016. *SANS 4001-BT1: Civil engineering specifications-Part BT1: Penetration grade bitumen*. Pretoria.

- [18] AASHTO T 312, 2015. *Standard method of test for preparing and determining the density of Hot Mix Asphalt (HMA) specimens by means of the Superpave gyratory compactor*. American Association of State and Highway Transportation Officials (AASHTO), Washington D.C.
- [19] ASTM D4867M, 2009. *Standard Test Method for Effect of Moisture on Asphalt Concrete Paving Mixtures*. West Conshohocken, PA: ASTM International.
- [20] AASHTO T 324, 2014. *"Method of Test for Hamburg Wheel-Track Testing of Compacted Hot Mix Asphalt (HMA)"*. American Association of State Highway and Transportation Officials, Washington D.C.
- [21] Anochie-Boateng, J.K. & George, T.B., 2016. Use of Waste Crushed Glass for the Manufacturing of Hot Mix Asphalt. In *4th International Conference on Sustainable Construction Materials and Technologies*. Las Vegas, USA.
- [22] NCHRP Project 20-07/Task 361, 2015. *Hamburg Wheel-Track Test Equipment Requirements and Improvements to AASHTO T 324*. Washington, D.C: Transportation Research Board.
- [23] Aschenbrener, T., 1995. Evaluation of Hamburg Wheel-Tracking Device to Predict moisture Damage in Hot Mix Asphalt. *Transportation Research Record*, 1492, pp.193-201.